JGR Oceans

RESEARCH ARTICLE
10.1029/2022JC018557

Sea Spray Impacts on Tropical Cyclone Olwyn Using a Coupled Atmosphere-Ocean-Wave Model

Xingkun Xu[1,2], Joey Jeff Voermans[1], Il-Ju Moon[3], Qingxiang Liu[1,4], Changlong Guan[2,4], and Alexander V. Babanin[1]

[1]Department of Infrastructure Engineering, University of Melbourne, Melbourne, VIC, Australia, [2]College of Oceanic and Atmospheric Sciences, Ocean University of China, Qingdao, China, [3]Typhoon Research Center, Jeju National University, Jeju, Korea, [4]Physical Oceanography Laboratory, Ocean University of China, Qingdao, China

Key Points:

- Implementation of wind-wave dependent sea spray parameterizations into the atmosphere-ocean-wave coupled model
- The simulation error of U_{10} and H_s for tropical cyclone (TC) Olwyn is significantly reduced by introducing the sea spray
- The sea spray plays a critical role in the development and intensification of TC Olwyn, and underlying sea surface temperature cooling

Supporting Information:

Supporting Information may be found in the online version of this article.

Correspondence to:

X. Xu,
xingkun.xu@student.unimelb.edu.au

Citation:

Xu, X., Voermans, J. J., Moon, I.-J., Liu, Q., Guan, C., & Babanin, A. V. (2022). Sea spray impacts on Tropical Cyclone Olwyn using a coupled atmosphere-ocean-wave model. *Journal of Geophysical Research: Oceans*, *127*, e2022JC018557. https://doi.org/10.1029/2022JC018557

Received 16 FEB 2022
Accepted 10 AUG 2022
Corrected 3 DEC 2022

This article was corrected on 3 DEC 2022. See the end of the full text for details.

Author Contributions:

Conceptualization: Xingkun Xu
Data curation: Xingkun Xu
Formal analysis: Xingkun Xu
Funding acquisition: Alexander V. Babanin
Investigation: Xingkun Xu
Methodology: Xingkun Xu

Abstract Extreme marine weather enhances the production of sea spray droplets which, in turn, affect the air-sea fluxes. Despite the ability of sea spray to modulate air-sea interaction processes, it remains under-represented in tropical cyclone (TC) forecasting modeling. In this study, impacts of sea spray on the atmospheric and oceanic environments of TC Olwyn are investigated. This is achieved by high-resolution nested simulations using an air-sea-wave model coupled with a sea spray production model. We compared two different sea spray models: a wave-Reynolds-number-dependent model, and a wave-steepness-dependent spray model. By including a sea spray model, the root mean square error in the simulated TC Olwyn 10 m wind and significant wave height are significantly reduced by up to 30% and 26%, respectively, in comparison to the baseline simulation without spray. This improvement is because sea spray decreases air-sea heat fluxes at larger radii of TC, and decreases air-sea heat fluxes at smaller radii of TC. In contrast to the simulated results without sea spray, sea spray increases the air-sea heat (sensible + latent) energy transfer and intensifies TC Olwyn. Sea spray also triggers stronger upper-ocean mixing and strengthens the TC-induced sea surface temperature cooling. Our results thus imply that sea spray critically impacts the atmosphere and ocean conditions during extreme marine weather and thus needs to be considered explicitly in TC forecasting modeling.

Plain Language Summary Large quantities of sea spray droplets are generated at the ocean surface and released into the air under extreme marine weather conditions. Even though sea spray plays an important role in the transfer of heat, moisture, and momentum between the air and ocean surface, its true impact remains uncertain in tropical cyclone (TC) modeling. In this study, we include a novel description of sea spray generation into an atmosphere-ocean-wave coupled model to investigate the impacts of sea spray on the development of TC Olwyn. In comparison to a simulation without sea spray, the errors of wind speed and wave height of the modeled TC Olwyn are considerably reduced when sea spray is considered. This improvement is expected to be from the impacts of sea spray on the structure of the TC Olwyn. As sea spray has significant effects on the atmospheric and oceanic environments, our results suggest that sea spray generations need to be included in current TC forecasting models.

1. Introduction

While tropical cyclone (TC) track forecasts have improved over the last three decades, the mean absolute errors of TC intensity forecasts have stagnated (Chan & Kepert, 2010; Emanuel, 2018; Palmer & Hagedorn, 2006; Rappaport et al., 2009; Warner, 2010). One of the primary reasons is the lack of sufficient understanding of the basic physical mechanisms that generate, drive, and maintain TCs (Chan, 2005; Chan & Kepert, 2010; Elsner et al., 2008). In particular, one external physical process that might affect the intensity of a TC is sea spray (Andreas & Emanuel, 2001; Gall et al., 2008; Xu, Voermans, Liu, et al., 2021).

Sea spray is composed of small water drops ejected from the ocean surface (Veron, 2015) and is of great significance for TC dynamics (Liu et al., 2011). For example, during extreme marine weather, spray droplets generated at the surface are strongly accelerated in the airflow and then return to the ocean surface, thus mediating the transfer of air-sea momentum (Donelan, 1990). In addition to dynamic effects, sea spray can also impact the air-sea heat fluxes through evaporation (Andreas & Emanuel, 2001). It was reported that sea spray induced heat fluxes are expected to account for more than 10% of the total air-sea heat and momentum fluxes once wind speed (WSP) reaches 11–13 m s^{-1} (Andreas, 2004; Andreas et al., 2008). As sea spray has significant thermal and dynamical

Project Administration: Alexander V. Babanin
Resources: Xingkun Xu
Software: Xingkun Xu
Supervision: Joey Jeff Voermans, Changlong Guan, Alexander V. Babanin
Validation: Xingkun Xu
Visualization: Xingkun Xu
Writing – review & editing: Xingkun Xu, Joey Jeff Voermans, Il-Ju Moon, Qingxiang Liu

effects on the air-sea interaction and thus TC dynamics, it needs to be clearly understood, parameterized and carefully implemented into TC modeling. In this study, we will implement two different sea spray parameterizations into a coupled air-sea-wave model.

Several studies have implemented sea spray parameterizations into operational numerical models to investigate the influence of sea spray on TC modeling. Wang et al. (2001) adopted a high-resolution TC model with explicit cloud microphysics to test the potential effects of sea spray on the TC intensity and maximum WSP. Gall et al. (2008), who utilized the non-hydrostatic MM5 (version 3.4), investigated the effects of sea spray on the TC's vertical structure within an idealized environment. These studies substantiated that sea spray, through moistening near-surface layers and altering their temperature, modifies the TC structure in important but complex ways. More recently, studies attempted to use regional coupled models to investigate effects of sea spray on TC modeling (Garg et al., 2018; Zhao et al., 2017). However, although the aforementioned studies have provided insights into how sea spray affects TC modeling, one of the foremost and common limitations in their studies is the choice of sea spray parameterization in TC modeling. For example, spray parametrizations utilized by current studies tend to be formulated in terms of the wind properties alone, either through the WSP or wind stress. It is intuitive to construct a sea spray model on the basis of wind characteristics, as the wind stress acting at the ocean surface can tear water liquid from the wave crests to form droplets. However, form properties of the ocean surface cannot be ignored in such a description (Laussac et al., 2018; Lenain & Melville, 2017; Ovadnevaite et al., 2014) for the simple reason that sea spray is unlikely to be produced (or at least at negligible quantities) when a perfectly horizontal ocean surface is considered, even during extreme winds (Xu, Voermans, Liu, et al., 2021). Thus, sea spray models need to be parameterized in terms of both wind and wave properties.

As a proxy of wave effects on sea spray generation, a Reynolds number was parameterized into a sea spray generation model (Zhao & Toba, 2001; Zhao et al., 2006; Norris et al., 2013),

$$V_{\mathrm{sp}} = \frac{4}{3}\pi \cdot \rho_w \int_{r_1}^{r_2} r^3 \cdot \frac{\mathrm{dF}(R_B)}{\mathrm{dr}}\mathrm{dr} \tag{1}$$

where V_{sp} is the sea spray volume flux; ρ_w is the water density; r is the radii of sea spray droplets; r_1 and r_2 are the radii of smallest and largest sea spray droplets; $\mathrm{dF}(R_B)/\mathrm{dr}$ is a wave-Reynolds-number-dependent sea spray generation function (see Equation 17 in Zhao et al. (2006)). Equation 1 was in turn, implemented into the coupled atmosphere–wave–ocean modeling system (Liu et al., 2011) and POMgcs-SWAN model (Zhang et al., 2017, 2021), respectively. While wave Reynolds number is a critical metric for wind-wave interaction, it has severe limitations in representing sea spray generation. For example, the wave Reynolds number, which is defined as the product of wind stress and wave age, cannot completely capture the properties of the ocean wave state. This is because wave age provides information on the relative velocity of the dominant energetic wave with respect to the wind only, but not about the severity of the sea state, including wave breaking. The severity of the sea state is considered to be a major determinant of sea spray generation (e.g., Bruch et al., 2021).

Recently, Xu, Voermans, Ma et al. (2021) derived a nondimensional wave-steepness-dependent sea spray volume flux parameterization based on WSP and wave steepness:

$$\frac{V_{\mathrm{sp}}}{U_{10}} = 1.99\sqrt{s} \times 10^{-8} \tag{2}$$

where U_{10} is the 10 m height WSP; $s = H_s k_m/2$ is the mean wave steepness, H_s is the significant wave height, and given at deep and shallow water $k_m = (2\pi f_m)^2/g$ and $k_m = 2\pi f_m/\sqrt{gh}$ is the mean wave number, respectively, where the f_m is the mean wave frequency and the g is the acceleration gravity. Using field observations of laser backscatter to parameterize the sea spray model, the model of Xu, Voermans, Ma et al. (2021) was found to perform remarkably similar to the model of Andreas (1992), both in trend and magnitude, when compared against the mean WSP. Notably different, however, is that the model of Andreas (1992) does not explicitly depend on the properties of the wave field. Therefore, we adopted Equations 1 and 2, respectively, to consider how the spray contributes to the air-sea interaction and implemented in TC modeling.

To simulate TCs, atmosphere numerical models are traditionally employed. However, in addition to the atmosphere, the underlying ocean should be simultaneously taken into account for TCs modeling as TCs develop over

the warm ocean and are sensitive to temporal variations of thermodynamic fluxes over the ocean surface and thus sea surface temperature (SST) changes (Bao et al., 2000). Without the coupling of the atmosphere and ocean, the negative feedback from the ocean to the atmospheric system at the air-sea interface would be missing, and the ocean would be functioned as an unlimited energy source for the intensification of TCs (Mogensen et al., 2017). By coupling the atmosphere with the ocean, sea surface cooling caused by TCs' passing results in a significant reduction of the TCs' intensity (Bao et al., 2011; Bender et al., 1993; Chan et al., 2001; Schade & Emanuel, 1999). As surface waves modulate the fluxes between the ocean and atmosphere, their influence needs to be accurately represented as well in the TC models. The role of waves in a coupled air-sea system is typically considered through an average roughness length and is closely related to the surface wind stress (Garratt, 1994; Kraus & Businger, 1994). As current numerical model analysis and observations suggested, the surface wind stress is not solely defined by the wind, but instead depends on both wind and wave states (Janssen, 1989). As the wind stress is associated with the energy supply from the ocean for TCs' development, the surface wave state needs to be considered in TC modeling. As such, a fully coupled atmosphere-ocean-wave model is required to simulate the life cycle of TCs (Bao et al., 2000; Mogensen et al., 2017).

This present work uses an air-sea-wave coupled numerical model to simulate TC Olywn at the North-West shelf of Australia in March 2015. To understand how sea spray mediates the air-sea interaction within the TC environment, we extended a bulk microphysical algorithm of Andreas et al. (2008) with the wave-Reynold-number- and wave-steepness-dependent sea spray models of Zhao et al. (2006) and Xu, Voermans, Ma et al. (2021) (we refer to these models as Z06 and X21 hereafter), respectively, to characterize the air-sea interaction processes at the ocean surface. We note, that this is the first study investigating the effects of sea spray on the TC dynamics using a fully coupled atmosphere-ocean-wave model in the Southern Hemisphere.

2. Methodology

2.1. TC Olwyn

To study the influences of the sea spray on the atmospheric and oceanic environments under extreme conditions, we here focus on the simulation of TC Olwyn for which in situ observations are available (Voermans et al., 2019). TC Olwyn developed as a tropical low-pressure system embedded in an intensive monsoon trough and moved to the northwest of Australia continental shelf (13.8°S, 115.6°E), before moving south from 10 March 2015. While slowly strengthening, this tropical low pressure system kept a southern track before reaching TC intensity at around 06:00/11/03. TC Olwyn passed by the observation site (19.58°S, 116.14°E) at a distance of 150 km at around 08:00/12/13, from where observed wind and wave properties are adopted to validate the simulations later on in this study. Then, it attained a minimum central sea level pressure (SLP) and peak intensity of around 75 knots (i.e., 139 km hr^{-1}) around 18:00/12/03. After that, the center of TC Olwyn passed west of Coral Bay, turned and moved toward the southeast, weakened to below TC intensity, and finally made landfall.

2.2. Description of Coupled Model

To simulate the life cycle of the TC Olwyn before its landfall, we adopted the fully Coupled Ocean-Atmosphere-Wave-Sediment Transportation numerical model system (COAWST) (Warner et al., 2010). COAWST consists of three components: the Weather Research Forecasting (WRF; https://www.wrf-model.org/plots/wrfrealtime.php) for the atmosphere (Skamarock et al., 2008), the Regional Ocean Modeling System (ROMS; https://www.myroms.org) for the ocean (Haidvogel et al., 2008; Shchepetkin & McWilliams, 2005, 2009), and the Simulating Wave Nearshore (SWAN) model for the waves (Booij et al., 1999; Warner et al., 2008). As these three components utilize a variety of prognostic variables in order to solve the governing equations, respectively, we briefly clarify the setup for each of them in more detail below.

2.2.1. Atmosphere

The atmosphere model used in COAWST is WRF with Advanced Research WRF core which, as a fully flexible and non-hydrostatic numerical model, integrates Euler equations by Arakawa-C grid using a terrain-following coordinate in vertical. In the present work, we set up two nested geographical atmospheric domains (Figure 1) with a horizontal resolution of 7.5 km for D01 and 1.5 km for D02, both of which contain 59 sigma levels. In this study, the initial field data and lateral boundary conditions were acquired from European Centre for

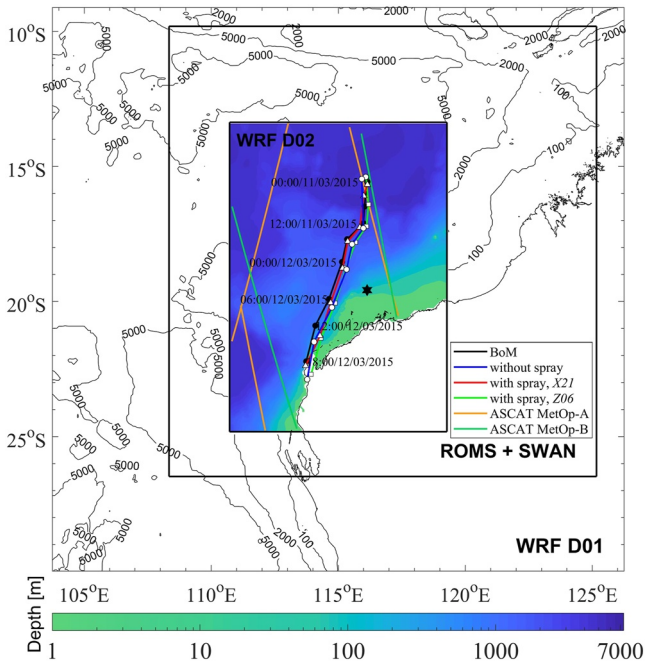

Figure 1. Atmosphere (Weather Research Forecasting (WRF (WRF)-Advanced Research WRF (ARW)), ocean (Regional Ocean Modelling System (ROMS)), and wave (Simulating Wave Nearshore (SWAN)) model domains. With WRF, the innermost domain (WRF D02) is nested within the outermost domain (WRF D01). ROMS and SWAN share the same domain (ROMS + SWAN). The tropical cyclone trajectory of simulations with the Z06 (solid green line), the X21 (solid red line), without sea spray (solid blue line), and the best-track observation of Bureau of Meteorology (BoM) (black solid line), respectively. The location of the fixed observation platform is presented by the black hexagram. Yellow and green solid lines are advanced scatterometers (ASCAT MetOp-A and ASCAT MetOp-B) passages. The shaded contours represent local bathymetry.

Medium-Range Weather Forecasts (European Centre for Medium-Range Weather Forecasts) produced the fifth generation atmospheric reanalysis (ERA-5) with a horizontal resolution of 0.25° × 0.25°.

2.2.2. Ocean

To provide ocean properties used in the bulk spray algorithm and consider oceanic responses during Olwyn passing, ROMS is defined as the ocean component in COAWST. ROMS is a free-surface numerical model using terrain-following coordinate to solve Reynolds-averaged Navier-Stokes with the hydrostatic and Boussinesq approximation (Shchepetkin & McWilliams, 2005). A model domain with 5 km horizontal resolution was used in this study (Figure 1). Vertically, the model domain utilized 30 levels for the extended terrain-following coordinate. For improving the computational efficiency and effectiveness nearshore during TC passing, the stretching parameters were chosen in case that the first sigma level was larger than 5 m. In this study, ROMS utilizes the field data of salinity (salt), temperature (temp), currents (U, V), averaged currents vertically (ubar, vbar), and sea surface level (zeta) to acquire initial conditions based on the outputs of global Hybrid Coordinate Ocean Model (HYCOM) GLBa0.08 from part of the United States Global Ocean Data Assimilation Experiment. The open boundary conditions for salinity, temperature, and current were also derived from the same database (https://tds.hycom.org/thredds/catalog.html).

2.2.3. Wave

SWAN, the wave model for the estimations of wave properties in the coastal area, is defined as the wave component in COAWST. In this study, SWAN adopted the same model simulation domain and grids with ROMS to save computational resources by reducing the time of transmission of grid data re-computation (Figure 1). Thirty six directions were obtained by determining the directional resolution as 10°. By defining the minimum frequency as 0.04 Hz, 24 frequencies were obtained. The initial conditions were from outputs of SWAN forced by WRF-ARW with the same computation grids and domain used in this study. The boundary conditions were from global simulation outputs of the WaveWatch III model (https://polar.ncep.noaa.gov/pub/history/waves).

To couple with wave and ocean components in COAWST system, the Model Coupling Toolkit is used as the coupling tool where these components mutually exchange information every time step (600 s), before they independently integrate forward for another coupling time step.

2.3. Sea Spray Effects

In COAWST, the Monin-Obukhov theory is implemented as the classic bulk turbulent flux algorithm to be used for estimating the air-sea fluxes. To obtain complete air-sea fluxes, in addition to air-sea turbulent fluxes, sea spray induced fluxes need to be considered. Here we adopt the spray flux algorithm developed by Andreas et al. (2008) who parameterized the air-sea fluxes with not only the air-sea turbulence but also sea spray. Therefore, we followed Andreas and Emanuel (2001); Andreas (2003), and adopted the methods of William Perrie (2004); Perrie et al. (2005) who replaced the default bulk flux algorithm with the bulk spray flux algorithm of Andreas et al. (2008).

In Andreas et al. (2008), air-sea total momentum τ_T fluxes, latent heat $H_{l,t}$, and sensible heat $H_{s,t}$ can be determined by the summation of the spray induced momentum τ_{sp}, latent heat $H_{l,sp}$, and sensible heat $H_{s,sp}$ fluxes and air-sea interfacial turbulent fluxes:

$$\tau_T = \tau + \tau_{sp} \quad (3)$$

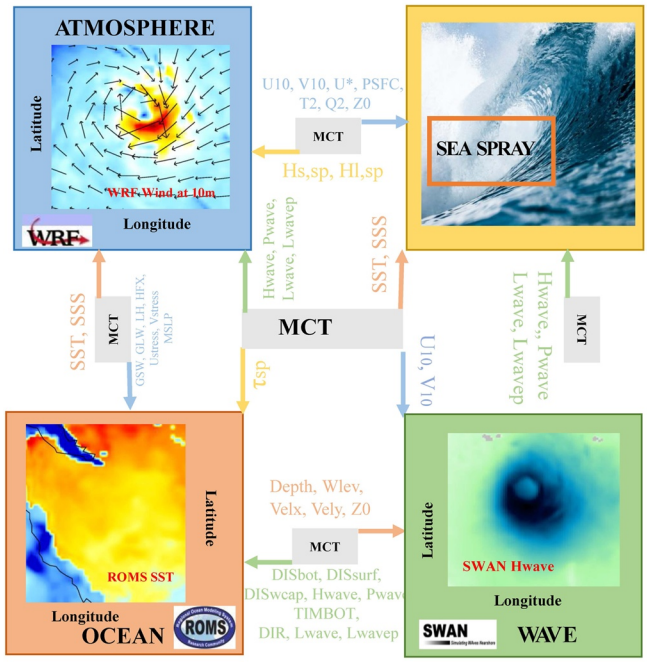

Variables	Description
GSW, GLW $[W \cdot m^2]$	Surface short, and long wave radiation
LH, HFX $[W \cdot m^{-2}]$	Surface latent, and sensible heat fluxes
Ustress, Vstress $[N \cdot m^{-2}]$	Surface U- and V- wind stress
MSLP $[Pa]$	Mean sea level pressure
SST $[°C]$	Sea surface temperature
U10, V10 $[m \cdot s^{-1}]$	U- and V- wind speed at 10 meter
U* $[m \cdot s^{-1}]$	Friction velocity
T2 $[°C]$	Surface 2-m air temperature
Q2 $[kg \cdot kg^{-1}]$	Water vapor mixing ratio at 2 meter
Z0 $[m]$	The roughness length
Hs,sp, HL,sp $[W \cdot m^{-2}]$	Sea spray induced sensible and latent heat fluxes
DISbot, DISsurf, DISwcap $[W \cdot m^{-2}]$	Energy dissipation due to bottom friction, surf-breaking and white-capping
Hwave $[m]$	Significant wave height
Pwave $[s]$	Peak wave period
TIMBOT $[s]$	Bottom wave period
DIR [°]	Wave direction
Lwave, Lwavep $[m]$	Mean and peak wavelength
Depth, Wlev $[m]$	Water depth and water level
Velx, Vely $[m \cdot s^{-1}]$	U- and V- current velocity

Figure 2. A schematic diagram of the atmosphere-ocean-wave-spray configurations and data fields exchange. τ_{sp}, $H_{l,sp}$, and $H_{s,sp}$ are the spray induced momentum latent heat and sensible heat fluxes, respectively (see Equations 3–5). For more details regarding the other coupling parameters and exchanges between each of the components, we refer to Warner et al. (2010); Xu, Voermans, Liu et al. (2021).

$$H_{l,t} = H_l + H_{l,\mathrm{sp}} \tag{4}$$

$$H_{s,t} = H_s + H_{s,\mathrm{sp}} \tag{5}$$

To introduce wave impacts on sea spray, we extrapolated the unique wave-steepness-dependent spray model proposed by Xu, Voermans, Ma et al. (2021) (Equation 1) to 45 m s^{-1} and substituted Equations 1 and 2, respectively, for the wind-dependent spray generation model already implemented in the bulk microphysical algorithm of Andreas (1992); Andreas et al. (2008) in this study for the modeling. As such, the coupled atmosphere-ocean-wave-spray system used in this study can be constructed (Figure 2).

3. Results

3.1. Wind Field, Wave Properties, and TC Olwyn

Figure 3 compares wind and wave observations obtained from the offshore platform (Voermans et al., 2019) with simulation results. In Figure 3a, both simulations with and without sea spray are similar and compare well with the observations when 10 m WSP (U_{10}) is less than around 15–20 m s^{-1}, whereas considerable differences are observed once U_{10} larger than around 15–20 m s^{-1}. In contrast to the simulated result without sea spray, including sea spray through Z06 and X21 reduces the root mean square error (RMSE) by about 28% and 30%, respectively, over the period from 16:00/10/03 to 18:00/12/03. Specifically, this improvement is most significant between 20:00/11/03 and 04:30/12/03 where U_{10} decreased by up to 2 and 3.5 m s^{-1} with Z06, and with X21, respectively. We note that such improvements are consistent when comparing our simulation results against observations by scatterometers (Figure S1 in Supporting Information S1). In Figure 3b, simulations of significant wave height (H_s) including Z06, and X21, and without sea spray are comparable and largely consistent with the observations when H_s is less than around 5 m. However, simulated H_s is decreased by up to 1.5 and 1.8 m considering Z06 and X21, respectively. The substantial improvements become noticeable at around 02:30/12/03 where the RMSE of H_s is reduced by about 20% and 25% when the sea spray models of Z06 and X21 are included, respectively.

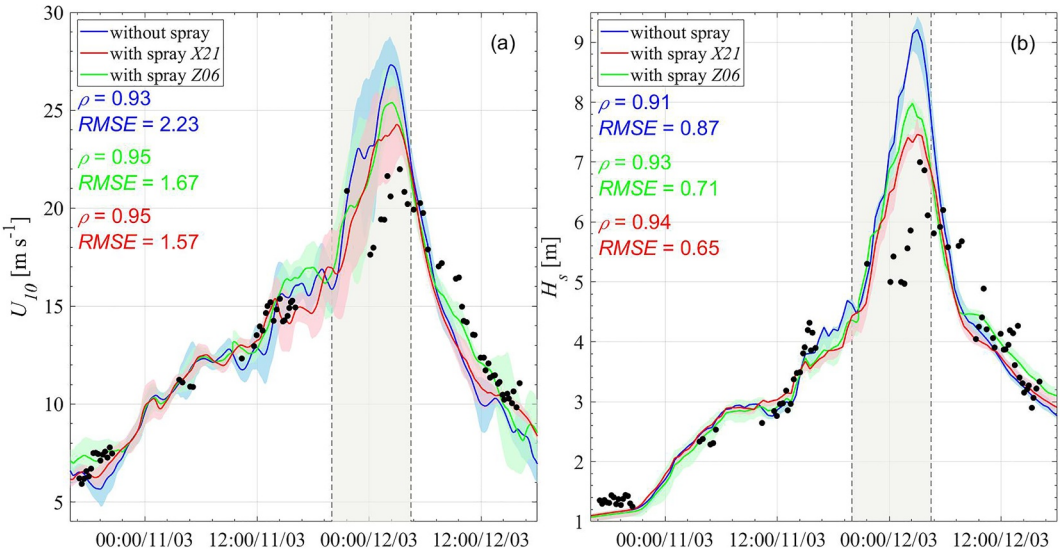

Figure 3. Comparison between (a) simulated wind speed at 10 m height, U_{10}, and (b) significant wave height, H_s, with observations from the fixed offshore platform (Voermans et al., 2019). The green, red and blue refer to simulation results with the Z06, with the X21 and without sea spray, respectively. Color bands represent the average value of grid points adjacent to the platform. Black dots are observations from the observational site. Areas where simulated U_{10} and H_s with the sea spray considerably differ from that without the sea spray are highlighted by gray shadows.

Figures 4a–4c compare the simulated TC track, SLP and maximum surface WSP following the center of TC Olwyn against observations from the Australian BoM. We note that, in the comparison with the observation, while the TC simulation without spray is considerably less intense, introducing sea spray reduces the deviation from the observation. Specifically, incorporating the sea spray models of Z06 and X21 contributes to the

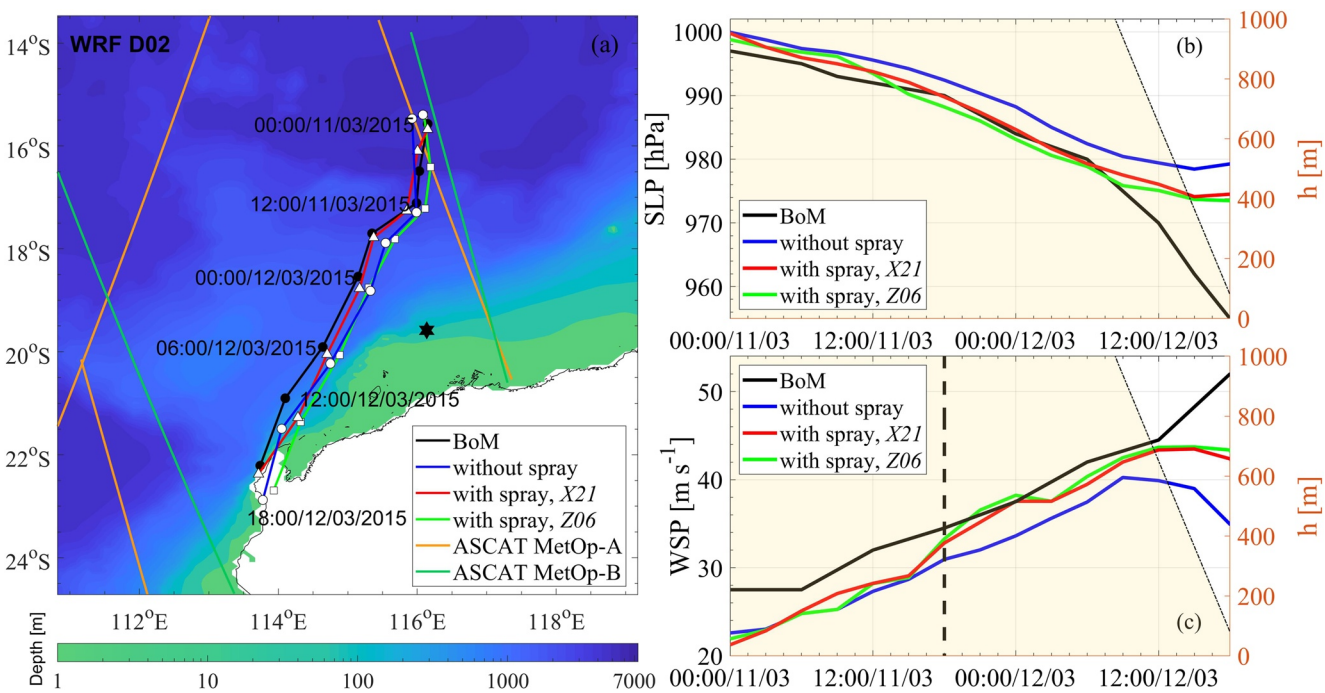

Figure 4. (a) The D02 of the Weather Research Forecasting (WRF) with the tropical cyclone (TC) tracks (as in Figure 1). (b) The minimum sea level pressure and (c) the maximum wind speed. The black, red and blue solid lines present the observation of Bureau of Meteorology (BoM), simulations with the sea spray models of Z06 and X21, and without sea spray, respectively. The black dashed line identifies the time when the simulation with sea spray considerably differs from that without sea spray. In each plot, the shadow region represents the local water depth nearby the TC center.

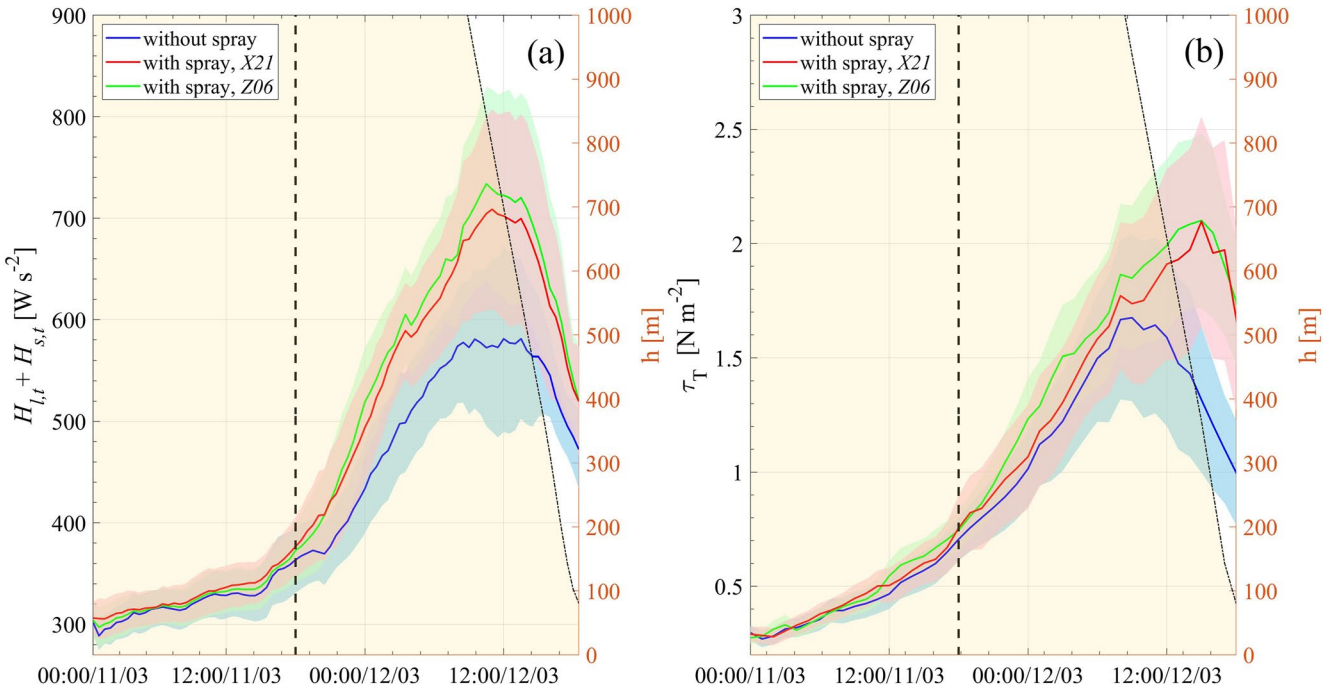

Figure 5. (a) The total air-sea heat fluxes (i.e., $H_{l,t} + H_{s,t}$) and (b) the momentum flux, τ_T. The red and blue are simulation results with the sea spray models of Z06 and X21, and without sea spray, respectively. Solid lines present the average of fluxes (i.e., heat fluxes for (a), and momentum fluxes for (b)) within two times of the radii of maximum wind from the center of tropical cyclones (TCs) for the simulation with sea spray and without sea spray, respectively. The color bands state their standard deviation estimations. The black dashed line is the time when the simulation with sea spray starts being largely deviating from that without sea spray. In each plot, the shadow region represents the local water depth at the TC center.

increase of maximum WSP by up to 8.4 and 5 m s^{-1}, respectively, at around 00:00/12/03. In agreement with the maximum WSP, in-time SLP is decreased by up to 8 and 7 hPa once the models of Z06 and X21 are considered, respectively. In line with other studies, our observations show that the inclusion of sea spray physics improves model performance and thus suggests that sea spray generation is a critical function in TC dynamics (Andreas & Emanuel, 2001; Kepert et al., 1999; Liu et al., 2011; Wang, 2009). After 06:00/12/03, TC Olwyn entered shallow water (less than 100 m), and it is responsible for the large differences between the simulation and BoM observations. As the energy supply from the ocean to the TC is abruptly cut off when the TC approaches the coastal zone, this destroys the TCs' warm-center vortex structure and complicates the physical and numerical processes at the underlying surface of the TC system. Therefore, to improve the simulation of TC entering shallow water, additional physical processes (i.e., nonbreaking-wave-induced turbulent mixing, rainfall, etc.) require representation in the TC model.

Figure 5a shows the maximum of the total heat (latent + sensible) flux across the ocean surface with time. Before around 18:00/11/03, the simulated heat fluxes with and without sea spray are closely comparable. However, after approximately 18:00/11/03, the simulation of heat fluxes become greatly increased because of introducing sea spray. In comparison with the simulation without spray, the air-sea total heat fluxes are increased by about 54.42 and 47.7 W s^{-2} (11.2%), with a maximum increase of 161.5 (27.3%) and 138.3 W s^{-2} (23.4%) for the inclusion of sea spray through the models of Z06 and X21, respectively, at around 11:00/12/03 (Figure 5a). After 18:00/11/03, the instance at which the simulated heat fluxes with sea spray start being significantly larger than that without sea spray (dashed line in Figure 5a), the maximum WSP is noticeably raised in contrast to the simulation without spray at around the same time (Figure 4c). Notably, it is at this time (i.e., 18:00/11/03) that winds become larger than 30 m s^{-1}. This may suggest that sea spray can play a significant role in TC meteorology once U_{10} is larger than around 30 m s^{-1}, which is observed and substantiated by others (Andreas, 2004; Andreas et al., 2008; Veron, 2015).

In addition to air-sea heat fluxes, we note an increase in the air-sea total momentum flux once the sea spray is incorporated into the simulation. Specifically, the overall total momentum is increased by about 0.21 N m^{-2} (21.7%)

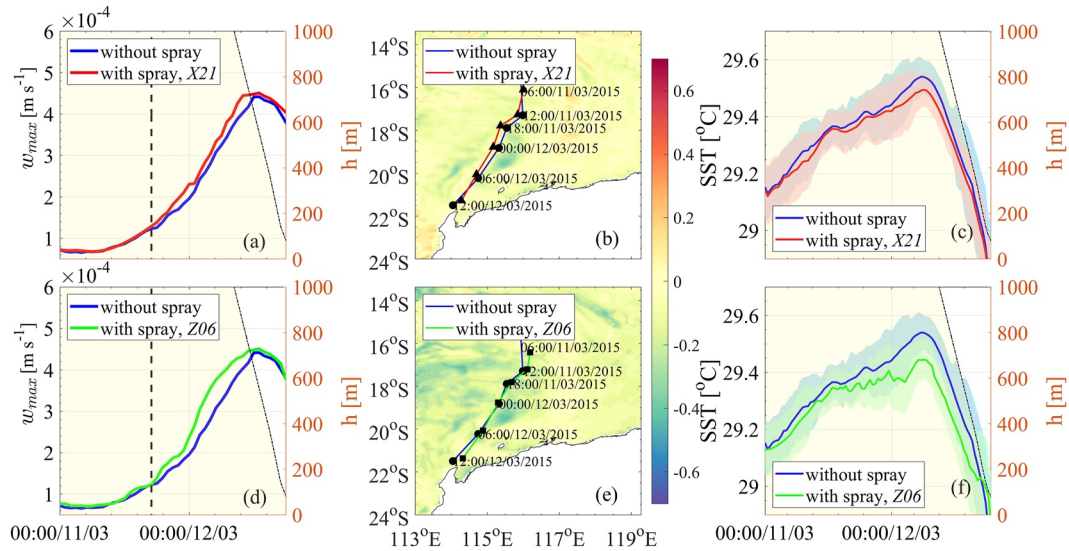

Figure 6. (a) and (d) The maximum vertical current velocity, w_{max}, at around 5 m depth below the sea surface following the tropical cyclone trajectory. (b and e) Spatial distributions for differences (i.e., the simulated sea surface temperature (SST) with spray minus that without spray) of SST at around 06:00/12/03 and (c and f) is the average of SST. The red, green, and blue present the simulation with sea spray given by Z06 and X21, and without sea spray, respectively. The color bands are their standard deviation estimations. The black dashed line demonstrates the time when the simulation with sea spray becomes deviating from that without sea spray.

and 0.16 N m^{-2} (16.1%) over the simulation time (Figure 5b) after the inclusion of Z06 and X21, respectively. The contribution of sea spray to the air-sea momentum fluxes becomes more evident from 18:00/11/03 onwards, which is consistent with the heat fluxes. A maximum of 0.87 N m^{-2} (79.2%) increase is observed at around 14:30/12/03 by introducing sea spray of X21, while a maximum of 0.84 N m^{-2} (69.6%) increase is observed at around 13:30/12/03 as a result of introducing sea spray of Z06. Thus, based on simulation results, the sea spray not only mediates the air-sea heat fluxes, but also the momentum fluxes.

3.2. Upper Ocean

Figures 6a and 6d show the comparison of maximum vertical current velocity, w_{max}, at around 5 m depth below the sea surface following the center of TC Olwyn between simulated results with and without sea spray. Both simulations suggest that w_{max} increases during Olwyn's intensification. Specifically, once the sea spray parameterizations of Z06 and X21 are included, respectively, the overall w_{max} is increased by 2.1 × 10^{-5} (9.8%) and 1.4 × 10^{-5} (6.2%) with a maximum of 7.5 × 10^{-5} (25.5%) and 4.1 × 10^{-5} (10.3%) at around 02:00/12/03 and 10:00/12/03. It is after approximately 18:00/11/03 that w_{max} increases more rapidly when sea spray is considered. We note that this corresponds to the time when sea spray effects on the heat fluxes are distinct in comparison to the baseline simulation without spray (e.g., see Figure 5a). As the sea spray adds additional kinetic energy to the upper ocean (Figure 5b), the vertical turbulent mixing and upwelling are expected to be enhanced as well. This contributes to stronger vertical turbulent mixing over the upper ocean, and thus a decrease of the SST is expected. Figures 6b and 6e present the SST differences (i.e., the simulated SST with sea spray minus that without sea spray) during the passage of Olwyn (see Figure S2 Supporting Information S1 for the SST in the experiment without and with spray, respectively). Sea spray induces widespread SST cooling distributed on both sides of TC Olwyn's trajectory. A maximum of about 0.31°C and 0.26°C cooling induced by Z06 and X21, respectively, occurs at around 12:00/12/03 (Figures 6c and 6f) along a narrow area to the left of the Olwyn's track (Figures 6b and 6e) because of the leftward bias of wind and wave fields. This is in agreement with previous studies (Perrie, 2004).

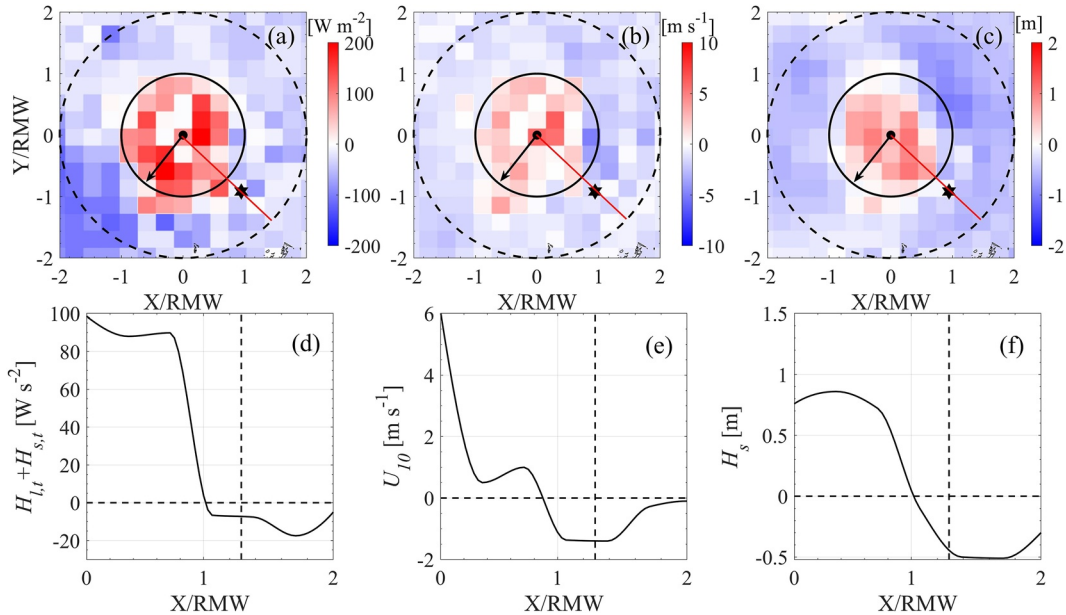

Figure 7. Spatial distribution of the difference between simulation with the X21 and without sea spray at 00:00/12/03 of (a) the total air-sea heat flux, (b) wind speed U_{10}, and (c) significant wave height H_s. (d–f) The profiles along the red lines as indicated in (a–c). The dashed-line circle in (a–c) is double the radii of maximum wind (RWM), the black solid-line circle is the RWM, and the arrow is the direction of tropical cyclone propagation in (a–c). The location of the fixed observation platform is presented by the black hexagram.

4. Discussion

In the present work, we investigated the impacts of sea spray on TC Olwyn through a coupled air-sea-wave model. In doing so, we have implemented a Reynolds-number-dependent and a unique wave-steepness-dependent sea spray model into the atmosphere-ocean-wave coupled system. We observe that by including sea spray into the air-sea-wave coupled model the simulated properties of wind and waves, that is, U_{10} and H_s, improve with respect to our field observations.

One of the foremost reasons for the improvements may be from impacts of sea spray on the TCs' structure. Here, we take the simulation including the model of X21 as an example to explain. At smaller radii (i.e., radii is approximately less than the radii of maximum wind (RWM)), the atmospheric sensible heat would be increased once sea spray droplets are ejected into the air. This is because the temperature of the generated sea spray, equal to the SST, is higher than the atmosphere, leading to sensible heat transfer from the sea spray to the surrounding air by conduction. Since the sea spray introduces additional sensible heat to the atmosphere, the total air-sea heat fluxes are, in turn, increased at smaller radii (Figure 7a). This contributes to the local increases of WSP (Figure 7b) and, subsequently, wave height (Figure 7c). However, at larger radii (i.e., radii is approximately larger than the RWM), sea spray droplets with smaller radii account for a substantial proportion of the amount generated sea spray (Gall et al., 2008). As sea spray droplets with smaller radii reside longer in the air (Andreas et al., 2008), the fraction of spray that evaporates increases, and occurs at the expense of the surrounding sensible heat (Andreas, 1992; Bao et al., 2000). This results in a decrease of the total air-sea heat fluxes, and potentially attenuates the intensity of local cyclones (Figures 7a and 7b). This is consistent with Gall et al. (2008), Barnes (2006), and Cione et al. (2000), the theoretical study of Andreas and Emanuel (2001) and the TCs modeling study conducted by Bao et al. (2000). As the fixed platform from which we obtained our field measurements is located at larger radii (see Figure S3 in Supporting Information S1), the simulated U_{10} and H_s at the platform location are reduced when sea spray is considered in comparison with the baseline simulation without sea spray (Figures 7b, 7c, 7e, and 7f). As such, in comparison with observations, introducing the sea spray improves the simulation of local winds and waves during TC Olwyn passing, and this is mainly from the tight coupling of sea spray, wind and waves, and the resulting impacts of sea spray on TC's structure.

In addition to the atmosphere and local waves, the impacts of sea spray on the ocean are also investigated in this study. Once the sea spray is considered, the upper ocean turbulent mixing is enhanced. This contributes to a deeper propagation of surface warm water downwards and greater upwelling of colder water resulting in SST cooling. We note that the SST cooling, with the maximum lying on the left/right side of the TC trajectory in the southern/northern hemisphere (see Figures 6b and 6e), occurs after the TC passing. This is because the temporal scale of the ocean is larger than that of the atmosphere, which contributes to the lagged effect of sea spray on the response of the upper ocean (see Figure S4 in Supporting Information S1). As this greater SST cooling is a result of introducing sea spray induced heat and momentum fluxes, we expect a positive feedback process between sea spray thermal and dynamical effects on the mediation of heat budget within the upper ocean (Zhang et al., 2017). That is, sea spray induced heat fluxes assist TC development and intensification which strengthen upwelling and SST cooling. In addition, the vertical turbulent mixing within the upper ocean is enhanced because of sea spray induced momentum fluxes. Given that TCs are one of the prominent upper ocean mixing agents at the global scale (Sriver & Huber, 2007), sea spray may be of significance to global climate and the marine biosphere by affecting upper ocean mixing, and thus the ability of the ocean to transport and store heat (Lin et al., 2003).

While our study shows that the inclusion of sea spray into the air-sea-wave coupled model improves the model performance in replicating the field observations, there are limitations in the sea spray parameterization of Xu, Voermans, Ma et al. (2021). First and foremost, the sea spray parameterization of Xu, Voermans, Ma et al. (2021) adopted here is restricted to wind speeds up to 25 m s^{-1} due to a lack of observations at higher WSP. The underlying assumption in this study is therefore that the parameterization is valid up to wind speeds of 45 m s^{-1} (see Figure S5 in Supporting Information S1 for the sensitive tests of the extrapolation of the sea spray parameterization of Xu, Voermans, Ma et al. (2021). Secondly, as the parameterization of Xu, Voermans, Ma et al. (2021) is developed based on field observations of laser backscatter, uncertainties may exist due to the modulation of laser attenuation by sea surface roughness properties as discussed by Xu, Voermans, Ma et al. (2021). Though further validation is required using laboratory, field and numerical observations, it is promising that this spray model, even when extrapolated to higher wind speeds, is well aligned with current sea spray models in both trend and magnitude (Xu, Voermans, Ma, et al., 2021). We further note that the extrapolation of sea spray models to extreme weather conditions in numerical models, as implied by Zhao et al. (2017) and Prakash et al. (2019), is commonly used and markedly improves the TCs modeling. However, further studies are required in reducing the uncertainty of the sea spray model used here at extreme wind speeds.

The air-sea-flux algorithm we utilized in this study is based on Andreas et al. (2008), who parameterized the evolution of sea spray in the air-sea layer using observations from the Humidity Exchange over the Sea experiment (DeCosmo et al., 1996; Katsaros et al., 1987; Smith et al., 1996), and the Fronts and Atlantic Storm-Tracks Experiment (Joly et al., 1997; Persson et al., 2005), two of the rare data sets at extreme winds. While this algorithm has been widely implemented in modeling for considerations of sea spray impacts on air-sea interaction (Garg et al., 2018; Liu et al., 2011; Prakash et al., 2019), uncertainties in this algorithm complicate estimates of the feedback effect of spray when depicting the evolution of sea spray in the air-sea layer (Troitskaya et al., 2018). Uncertainties include, but are not limited to, estimating the initial velocity of ejected drops from the ocean surface, and quantifying the fraction of spray drops that evaporate and fall back to the ocean. Therefore, further studies are required to understand the sea spray microphysics at the ocean surface and their evolution in the air, which may reduce the modeling errors further in extreme weather conditions.

Despite the uncertainties in sea spray dynamics, including sea spray into the TC model leads to a marked improvement, specifically, it reduced the simulation error of U_{10} and H_s for TC Olwyn with respect to the baseline simulation. While we see significant improvement for both the sea spray parameterizations, we note that both the sea spray models perform similar. As the model of X21 is based on the wave steepness, considered the critical parameter in the generation of sea spray (e.g. Bruch et al., 2021), the model of X21 is preferred over that of Z06. This study considers, however, only one TC case which reached up to category 3. More TC cases are required to be collected, simulated, and analyzed to generalize the findings described above. This is particularly true and required for operational purposes. Nonetheless, the presented study implies that the sea spray plays a critical role in the atmospheric and oceanic dynamics at extreme winds and it requires to be introduced into the operational models of the TC forecasting.

5. Conclusions

In this present work, we adopted an air-sea-wave coupled model with 1.5 km resolution to simulate the TC Olwyn. To investigate the influence of wind-wave driven sea spray on the air-sea interaction under strong winds, we replaced the model default bulk algorithm with a bulk spray flux algorithm. We adopted a wave Reynolds-number and wind-wave-steepness-dependent sea spray model, referred to as Z06 and X21 respectively.

In comparison with the baseline simulation, the introduction of the models of Z06 and X21 increases the air-sea total heat (sensible heat + latent heat) by about 12.8% and 11.2%, respectively, providing a supplemental energy source to support the development and intensification of TC Olwyn. By including dynamic effects of sea spray through the models of Z06 and X21, the air-sea momentum fluxes are increased by about 21.7% and 16.1%, respectively, with respect to that without sea spray. This enhances the turbulent mixing and upwelling on the upper ocean which, in turn, enhanced SST cooling, thereby strengthen the negative feedback from the ocean to the atmospheric system of the TC Olwyn. Consistent with the current study, we suggested a positive feedback process between the dynamic and thermal effects of sea spray on the heat budget within the upper ocean.

Incorporating the sea spray into the air-sea-wave coupled model improves prediction of local winds and waves. In the comparison of the simulations with the Reynolds-number and wave-steepness-dependent sea spray parameterizations and without sea spray, errors in RMSE are reduced by up to 30% and 26% for U_{10} and H_s, respectively. While both the sea spray models of Z06 and X21 improve the simulations significantly, the model of X21 seems to perform slightly better than Z06. Moreover, as the parameterization of X21 depends on the severity of the sea state, the physical relevance of X21 makes it a more suitable parameterization for implementation in the coupled models.

Results suggest that such improvements might come from the impacts of sea spray on the structure of TC Olwyn. That is, sea spray reduces the air-sea heat fluxes at larger radii of TC Olwyn, and increases the air-sea heat fluxes at smaller radii. The significant improvements in model results affirm the necessity of including sea spray physics into the TC operational forecasting. Future work requires the study of more TC cases in various categories to generalize the findings presented above.

Data Availability Statement

The data utilized in this study are available via https://figshare.com/articles/dataset/Datasets/20484342. The satellite data are available at the Australian Ocean Data Network (AODN) Portal. Data for the coupled model are available online from the ERA-5 (https://cds.climate.copernicus.eu/cdsapp#!/home), HYCOM analysis (http://tds.hycom.org/thredds/dodsC/GLBa0.08/expt_91.1), and WW3 outputs (ftp://polar.ncep.noaa.gov/pub/history/waves/).

Acknowledgments
X. Xu, J. Voermans, and A. Babanin acknowledge the support of the Centre of Disaster Management and Public Safety of the University of Melbourne. A. Babanin acknowledges support of the US Office of Naval Research Global, Grant Number N62909-20-1-2080. The authors are grateful to Woodside Ltd., and Australian Bureau of Meteorology (BoM) for giving access to the data. I. J. Moon acknowledged the support of the project titled "Establishment of the ocean research station in the jurisdiction zone and convergence research" funded by the Ministry of Oceans and Fisheries in Korea. The authors thank Prof. Sergey Suslov, A/Prof. Ivica Janekovic, Dr. Jeff Kepert for their support and discussion. Open access publishing is facilitated by The University of Melbourne, as part of the Wiley - The University of Melbourne agreement via the Council of Australian University Librarians.

References

Andreas, E. L. (1992). Sea spray and the turbulent air-sea heat fluxes. *Journal of Geophysical Research*, *97*(C7), 11429–11441. https://doi.org/10.1029/92jc00876

Andreas, E. L. (2003). 3.4 an algorithm to predict the turbulent air-sea fluxes in high-wind, spray conditions.

Andreas, E. L. (2004). Spray stress revisited. *Journal of Physical Oceanography*, *34*(6), 1429–1440. https://doi.org/10.1175/1520-0485(2004)034<1429:ssr>2.0.co;2

Andreas, E. L., & Emanuel, K. A. (2001). Effects of sea spray on tropical cyclone intensity. *Journal of the Atmospheric Sciences*, *58*(24), 3741–3751. https://doi.org/10.1175/1520-0469(2001)058<3741:eossot>2.0.co;2

Andreas, E. L., Persson, P. O. G., & Hare, J. E. (2008). A bulk turbulent air–sea flux algorithm for high-wind, spray conditions. *Journal of Physical Oceanography*, *38*(7), 1581–1596. https://doi.org/10.1175/2007jpo3813.1

Bao, J., Wilczak, J., Choi, J., & Kantha, L. (2000). Numerical simulations of air–sea interaction under high wind conditions using a coupled model: A study of hurricane development. *Monthly Weather Review*, *128*(7), 2190–2210. https://doi.org/10.1175/1520-0493(2000)128<2190:nsoasi>2.0.co;2

Bao, J.-W., Fairall, C. W., Michelson, S., & Bianco, L. (2011). Parameterizations of sea-spray impact on the air–sea momentum and heat fluxes. *Monthly Weather Review*, *139*(12), 3781–3797. https://doi.org/10.1175/mwr-d-11-00007.1

Barnes, G. M. (2006). Thermodynamic structure of a hurricane's lower cloud and subcloud layers. In *27th Conference on Hurricanes and Tropical Meteorology*. American Meteorological Society. paper presented at Preprints.

Bender, M. A., Ginis, I., & Kurihara, Y. (1993). Numerical simulations of tropical cyclone-ocean interaction with a high-resolution coupled model. *Journal of Geophysical Research*, *98*(D12), 23245. https://doi.org/10.1029/93jd02370

Booij, N., Ris, R. C., & Holthuijsen, L. H. (1999). A third-generation wave model for coastal regions: 1. Model description and validation. *Journal of Geophysical Research*, *104*(C4), 7649–7666. https://doi.org/10.1029/98jc02622

Bruch, W., Piazzola, J., Branger, H., van Eijk, A. M., Luneau, C., Bourras, D., & Tedeschi, G. (2021). Sea-spray-generation dependence on wind and wave combinations: A laboratory study. *Boundary-Layer Meteorology*, *180*(3), 477–505. https://doi.org/10.1007/s10546-021-00636-y

Chan, J. C., Duan, Y., & Shay, L. K. (2001). Tropical cyclone intensity change from a simple ocean–atmosphere coupled model. *Journal of the Atmospheric Sciences*, *58*(2), 154–172. https://doi.org/10.1175/1520-0469(2001)058<0154:tcicfa>2.0.co;2

Chan, J. C., & Kepert, J. D. (2010). Global perspectives on tropical cyclones: From science to mitigation.

Chan, J. C. L. (2005). The physics of tropical cyclone motion. *Annual Review of Fluid Mechanics*, *37*(1), 99–128. https://doi.org/10.1146/annurev.fluid.37.061903.175702

Cione, J. J., Black, P. G., & Houston, S. H. (2000). Surface observations in the hurricane environment. *Monthly Weather Review*, *128*(5), 1550–1561. https://doi.org/10.1175/1520-0493(2000)128<1550:soithe>2.0.co;2

DeCosmo, J., Katsaros, K., Smith, S., Anderson, R., Oost, W., Bumke, K., & Chadwick, H. (1996). Air-sea exchange of water vapor and sensible heat: The humidity exchange over the sea (HEXOS) results. *Journal of Geophysical Research*, *101*(C5), 12001–12016. https://doi.org/10.1029/95jc03796

Donelan, M. A. (1990). Air-sea interaction. *Sea*, *9*, 239–292.

Elsner, J. B., Kossin, J. P., & Jagger, T. H. (2008). The increasing intensity of the strongest tropical cyclones. *Nature*, *455*(7209), 92–95. https://doi.org/10.1038/nature07234

Emanuel, K. (2018). 100 years of progress in tropical cyclone research. *Meteorological Monographs*, *59*, 1511–1568. https://doi.org/10.1175/amsmonographs-d-18-0016.1

Gall, J. S., Frank, W. M., & Kwon, Y. (2008). Effects of sea spray on tropical cyclones simulated under idealized conditions. *Monthly Weather Review*, *136*(5), 1686–1705. https://doi.org/10.1175/2007mwr2183.1

Garg, N., Ng, E. Y. K., & Narasimalu, S. (2018). The effects of sea spray and atmosphere–wave coupling on air–sea exchange during a tropical cyclone. *Atmospheric Chemistry and Physics*, *18*(8), 6001–6021. https://doi.org/10.5194/acp-18-6001-2018

Garratt, J. R. (1994). The atmospheric boundary layer. *Earth-Science Reviews*, *37*(1–2), 89–134. https://doi.org/10.1016/0012-8252(94)90026-4

Haidvogel, D. B., Arango, H., Budgell, W., Cornuelle, B., Curchitser, E., Di Lorenzo, E., et al. (2008). Ocean forecasting in terrain-following coordinates: Formulation and skill assessment of the regional ocean modeling system. *Journal of Computational Physics*, *227*(7), 3595–3624. https://doi.org/10.1016/j.jcp.2007.06.016

Janssen, P. A. (1989). Wave-induced stress and the drag of air flow over sea waves. *Journal of Physical Oceanography*, *19*(6), 745–754. https://doi.org/10.1175/1520-0485(1989)019<0745:wisatd>2.0.co;2

Joly, A., Jorgensen, D., Shapiro, M. A., Thorpe, A., Bessemoulin, P., Browning, K. A., et al. (1997). The fronts and Atlantic storm-track experiment (FASTEX): Scientific objectives and experimental design. *Bulletin of the American Meteorological Society*, *78*(9), 1917–1940. https://doi.org/10.1175/1520-0477(1997)078<1917:tfaast>2.0.co;2

Katsaros, K. B., Smith, S. D., & Oost, W. A. (1987). HEXOS—Humidity exchange over the sea a program for research on water-vapor and droplet fluxes from sea to air at moderate to high wind speeds. *Bulletin of the American Meteorological Society*, *68*(5), 466–476. https://doi.org/10.1175/1520-0477(1987)068<0466:heotsa>2.0.co;2

Kepert, J., Fairall, C., & Bao, J.-W. (1999). Modelling the interaction between the atmospheric boundary layer and evaporating sea spray droplets. In *Air-sea exchange: Physics, chemistry and dynamics* (pp. 363–409). Springer.

Kraus, E. B., & Businger, J. A. (1994). *Atmosphere-ocean interaction*. Oxford University Press.

Laussac, S., Piazzola, J., Tedeschi, G., Yohia, C., Canepa, E., Rizza, U., & Van Eijk, A. M. J. (2018). Development of a fetch dependent sea-spray source function using aerosol concentration measurements in the North-Western Mediterranean. *Atmospheric Environment*, *193*, 177–189. https://doi.org/10.1016/j.atmosenv.2018.09.009

Lenain, L., & Melville, W. K. (2017). Evidence of sea-state dependence of aerosol concentration in the Marine atmospheric boundary layer. *Journal of Physical Oceanography*, *47*(1), 69–84. https://doi.org/10.1175/jpo-d-16-0058.1

Lin, I., Liu, W. T., Wu, C. C., Wong, G. T., Hu, C., Chen, Z., et al. (2003). New evidence for enhanced ocean primary production triggered by tropical cyclone. *Geophysical Research Letters*, *30*(13), 1718. https://doi.org/10.1029/2003gl017141

Liu, B., Liu, H., Xie, L., Guan, C., & Zhao, D. (2011). A coupled atmosphere–wave–ocean modeling system: Simulation of the Intensity of an Idealized Tropical Cyclone. *Monthly Weather Review*, *139*(1), 132–152. https://doi.org/10.1175/2010mwr3396.1

Mogensen, K. S., Magnusson, L., & Bidlot, J.-R. (2017). Tropical cyclone sensitivity to ocean coupling in the ECMWF coupled model. *Journal of Geophysical Research: Oceans*, *122*, 4392–4412. https://doi.org/10.1002/2017jc012753

Norris, S. J., Brooks, I. M., & Salisbury, D. J. (2013). A wave roughness Reynolds number parameterization of the sea spray source flux. *Geophysical Research Letters*, *40*(16), 4415–4419. https://doi.org/10.1002/grl.50795

Ovadnevaite, J., Manders, A., de Leeuw, G., Ceburnis, D., Monahan, C., Partanen, A. I., et al. (2014). A sea spray aerosol flux parameterization encapsulating wave state. *Atmospheric Chemistry and Physics*, *14*(4), 1837–1852. https://doi.org/10.5194/acp-14-1837-2014

Palmer, T., & Hagedorn, R. (2006). *Predictability of weather and climate*. Cambridge University Press.

Perrie, W. (2004). Simulation of extratropical Hurricane Gustav using a coupled atmosphere-ocean-sea spray model. *Geophysical Research Letters*, *31*(3), L03110. https://doi.org/10.1029/2003gl018571

Perrie, W., Zhang, W., Andreas, E. L., Li, W., Gyakum, J., & McTaggart-Cowan, R. (2005). Sea spray impacts on intensifying midlatitude cyclones. *Journal of the Atmospheric Sciences*, *62*(6), 1867–1883. https://doi.org/10.1175/jas3436.1

Persson, P. O. G., Hare, J., Fairall, C., & Otto, W. (2005). Air–sea interaction processes in warm and cold sectors of extratropical cyclonic storms observed during FASTEX. *Quarterly Journal of the Royal Meteorological Society: A Journal of the Atmospheric Sciences, Applied Meteorology and Physical Oceanography*, *131*(607), 877–912. https://doi.org/10.1256/qj.03.181

Prakash, K. R., Pant, V., & Nigam, T. (2019). Effects of the sea surface roughness and sea spray-induced flux parameterization on the simulations of a tropical cyclone. *Journal of Geophysical Research: Atmospheres*, *124*, 14037–14058. https://doi.org/10.1029/2018jd029760

Rappaport, E. N., Franklin, J. L., Avila, L. A., Baig, S. R., Beven, J. L., Blake, E. S., et al. (2009). Advances and challenges at the national hurricane center. *Weather and Forecasting*, *24*(2), 395–419. https://doi.org/10.1175/2008waf2222128.1

Schade, L. R., & Emanuel, K. A. (1999). The ocean's effect on the intensity of tropical cyclones: Results from a simple coupled atmosphere–ocean model. *Journal of the Atmospheric Sciences*, *56*(4), 642–651. https://doi.org/10.1175/1520-0469(1999)056<0642:toseot>2.0.co;2

Shchepetkin, A. F., & McWilliams, J. C. (2005). The regional oceanic modeling system (ROMS): A split-explicit, free-surface, topography-following-coordinate oceanic model. *Ocean Modelling*, *9*(4), 347–404. https://doi.org/10.1016/j.ocemod.2004.08.002

Shchepetkin, A. F., & McWilliams, J. C. (2009). Correction and commentary for "Ocean forecasting in terrain-following coordinates: Formulation and skill assessment of the regional ocean modeling system" by Haidvogel et al., J. Comp. Phys. 227, pp. 3595–3624. *Journal of Computational Physics*, *228*(24), 8985–9000. https://doi.org/10.1016/j.jcp.2009.09.002

Skamarock, W., Klemp, J., Dudhia, J., Gill, D., Barker, D., Wang, W., & Powers, J. (2008). *A description of the advanced research WRF version 3*. National Center for Atmospheric Research. Rep., NCAR Technical Note NCAR/TN-4751STR.

Smith, S. D., Katsaros, K. B., Oost, W. A., & Mestayer, P. G. (1996). The impact of the HEXOS programme. In *Boundary-layer meteorology 25th anniversary* (Vol. 1970–1995, pp. 121–141). Springer.

Sriver, R. L., & Huber, M. (2007). Observational evidence for an ocean heat pump induced by tropical cyclones. *Nature*, *447*(7144), 577–580. https://doi.org/10.1038/nature05785

Troitskaya, Y., Druzhinin, O., Kozlov, D., & Zilitinkevich, S. (2018). The "bag breakup" spume droplet generation mechanism at high winds. Part II: Contribution to momentum and enthalpy transfer. *Journal of Physical Oceanography*, *48*(9), 2189–2207. https://doi.org/10.1175/jpo-d-17-0105.1

Veron, F. (2015). Ocean spray. *Annual Review of Fluid Mechanics*, *47*(1), 507–538. https://doi.org/10.1146/annurev-fluid-010814-014651

Voermans, J. J., Rapizo, H., Ma, H., Qiao, F., & Babanin, A. V. (2019). Air–sea momentum fluxes during tropical cyclone olwyn. *Journal of Physical Oceanography*, *49*(6), 1369–1379. https://doi.org/10.1175/jpo-d-18-0261.1

Wang, Y. (2009). How do outer spiral rainbands affect tropical cyclone structure and intensity? *Journal of the Atmospheric Sciences*, *66*(5), 1250–1273. https://doi.org/10.1175/2008jas2737.1

Wang, Y., Kepert, J. D., & Holland, G. J. (2001). The effect of sea spray evaporation on tropical cyclone boundary layer structure and intensity. *Monthly Weather Review*, *129*(10), 2481–2500. https://doi.org/10.1175/1520-0493(2001)129<2481:teosse>2.0.co;2

Warner, J. C., Armstrong, B., He, R., & Zambon, J. B. (2010). Development of a coupled ocean–atmosphere–wave–sediment transport (COAWST) modeling system. *Ocean Modelling*, *35*(3), 230–244. https://doi.org/10.1016/j.ocemod.2010.07.010

Warner, J. C., Sherwood, C. R., Signell, R. P., Harris, C. K., & Arango, H. G. (2008). Development of a three-dimensional, regional, coupled wave, current, and sediment-transport model. *Computers & Geosciences*, *34*(10), 1284–1306. https://doi.org/10.1016/j.cageo.2008.02.012

Warner, T. T. (2010). *Numerical weather and climate prediction*. cambridge university press.

Xu, X., Voermans, J. J., Liu, Q., Moon, I.-J., Guan, C., & Babanin, A. V. (2021b). Impacts of the wave-dependent sea spray parameterizations on air–sea–wave coupled modeling under an idealized tropical cyclone. *Journal of Marine Science and Engineering*, *9*(12), 1390. https://doi.org/10.3390/jmse9121390

Xu, X., Voermans, J. J., Ma, H., Guan, C., & Babanin, A. V. (2021). A wind–wave-dependent sea spray volume flux model based on field experiments. *Journal of Marine Science and Engineering*, *9*(11), 1168. https://doi.org/10.3390/jmse9111168

Zhang, L., Zhang, X., Chu, P. C., Guan, C., Fu, H., Chao, G., et al. (2017). Impact of sea spray on the Yellow and East China seas thermal structure during the passage of typhoon Rammasun (2002). *Journal of Geophysical Research: Oceans*, *122*, 7783–7802. https://doi.org/10.1002/2016jc012592

Zhang, L., Zhang, X., Perrie, W., Guan, C., Dan, B., Sun, C., et al. (2021). Impact of sea spray and sea surface roughness on the upper ocean response to super typhoon Haitang. *Journal of Physical Oceanography*.

Zhao, B., Qiao, F., Cavaleri, L., Wang, G., Bertotti, L., & Liu, L. (2017). Sensitivity of typhoon modeling to surface waves and rainfall. *Journal of Geophysical Research: Oceans*, *122*, 1702–1723. https://doi.org/10.1002/2016jc012262

Zhao, D., & Toba, Y. (2001). Dependence of whitecap coverage on wind and wind-wave properties. *Journal of Oceanography*, *57*(5), 603–616. https://doi.org/10.1023/a:1021215904955

Zhao, D., Toba, Y., Sugioka, K.-I., & Komori, S. (2006). New sea spray generation function for spume droplets. *Journal of Geophysical Research*, *111*, C02007. https://doi.org/10.1029/2005jc002960

Erratum

The following open access funding statement was missing from the originally published version of this article: Open access publishing is facilitated by The University of Melbourne, as part of the Wiley - The University of Melbourne agreement via the Council of Australian University Librarians. The error has been corrected, and this may be considered the authoritative version of record.